THE ASTROPHYSICAL JOURNAL, 227:900–906, 1979 February 1

CIRCUMSTELLAR DUST ENVELOPES: CALCULATION OF ECLIPSE LIGHT CURVES AND FRINGE VISIBILITIES

DENNIS R. CRABTREE AND P. G. MARTIN
Department of Astronomy and David Dunlap Observatory, University of Toronto
Received 1978 June 22; accepted 1978 August 8

ABSTRACT

We describe a procedure by which the fringe visibility, as obtained by using a two-element Michelson interferometer, and an eclipse light curve, as observed during a lunar occultation, can be computed for models of extended circumstellar dust envelopes. The potential value of these measures of angular size in the interpretation of observed circumstellar regions is demonstrated by an investigation of their systematic dependence on various model parameters. An application to IRC +10216 suggests that a model involving two distinct components, such as is currently popular, may not be required to explain the observations.

Subject headings: infrared: sources — interferometry — occultations — stars: circumstellar shells

I. INTRODUCTION

Many late-type stars emit more radiation in the infrared than would be expected from a simple extrapolation of the observed optical flux. These infrared excesses have generally been attributed to thermal emission from warm dust particles in circumstellar envelopes (e.g., Woolf 1973). Interpretive models have ranged from simple addition of gray-body dust-shell spectra to stellar continua (e.g., Feast and Glass 1973) to more detailed attempts based on a self-consistent solution of the equations of radiative transfer in spherical geometry for the general nongray case (e.g., Jones and Merrill 1976).

The observed properties of a circumstellar envelope are dependent on the nature of the grain material, through the refractive index and particle size, and on the distribution of grains, through the opacity and equilibrium grain temperature. Unique characterization of an envelope is therefore problematical in the absence of extensive observational data. The most commonly available data are photometric measurements in the range 1–20 μm. Two complementary approaches have been taken. On the one hand, attempts have been made to match the detailed spectra for a few individual stars (e.g., Apruzese 1974, 1975; Taam and Schwartz 1976); on the other, spectra for grids of models in which input parameters are systematically varied have been computed for comparison with coarse spectrophotometric observations of a large number of stars (Jones and Merrill 1976; Robinson and Hyland 1977). It is clear, however, that a greater variety of observations will be needed to specify the nature of the envelopes accurately. The purpose of the present paper is to emphasize the inherent potential of observations of the spatial extent of these infrared sources. Although some such data already exist, little attention has been given to their analysis by using sophisticated envelope models.

Flux measurements, at several wavelengths, have been obtained for a few infrared sources during lunar occultations (Toombs *et al.* 1972; Zappala *et al.* 1974). Many more sources can be examined by using a two-element Michelson interferometer to establish the fringe visibility (Michelson and Pease 1921) as a function of element separation and/or wavelength (e.g., McCarthy and Low 1975; Sutton *et al.* 1977). A model characteristic common to the interpretation of these observations is the strip brightness distribution across the projected face of the source; in the former case we are interested in the integral of this distribution over the visible part of the source, whereas in the latter the Fourier transform of the distribution is utilized.

To calculate the strip brightness distribution, it is in general necessary to know the angular dependence of the specific intensity at each point on the surface of the envelope; a spherically symmetric envelope is an important special case in which the angular dependence at each surface point is equivalent. Prediction of the specific intensity has not been the purpose of most models of circumstellar envelopes; moments of the specific intensity, such as flux, have been regarded as more essential. However, the specific intensity is calculated explicitly in some numerical techniques, and is therefore available for exploitation.

In § II we describe one procedure by which the specific intensity, and the dependent observables, can be computed. The sensitivity to model parameters, particularly total optical depth and radial dependence of the density distribution, is explored in § III, with the conclusion that observations of the angular structure could play a pivotal role in the interpretation

of circumstellar envelopes. A preliminary application to IRC +10216 is presented in § IV.

II. MODEL CALCULATIONS

Like earlier models, ours consists of a central star emitting like a blackbody, surrounded by a spherically symmetric envelope containing dust particles. Many models which have addressed mainly the spectral dependence of the emergent radiation have also provided a self-consistent solution to the temperature distribution in the envelope. The temperature distribution is sensitive to the opacity of the envelope, the density distribution, and the choice of grain size and material. It is generally lower than the temperature distribution for an optically thin envelope, because of thermalization of the outflowing radiation. Since none of our shells are optically thin, the temperature distributions all fall below the optically thin limit. We have been content to adapt the appropriate temperature distributions in order to concentrate on the original aspects of this paper. Our work therefore extends earlier models by predicting the specific intensity at the surface. One check on the consistency of our results is that the integrated luminosity of the envelope and obscured central star is close to the intrinsic luminosity of the star.

Another area in which the temperature becomes important is in defining the inner edge of the envelope. We adopt the view that grains can exist wherever the calculated equilibrium temperature is below the condensation temperature for that material. An adequate approximation to the inner cutoff is obtained by using the temperature distribution for an optically thin envelope, in which each grain can be considered independent of the others. Allowance can be made for the angular dependence of the radiation field within a few stellar radii of the photosphere (Bergeat *et al.* 1976).

The fundamental calculation performed here is the integration of the specific intensity along individual rays through the envelope. Rays with different impact parameters correspond to different emergent angles at the surface, or, for our application, to different points on the projected face of the source. Because the temperature distribution is specified for a given grain distribution, and scattering is assumed to be negligible in the infrared, the source function is known at each point along the ray. The assumptions of spherical symmetry and negligible scattering in the infrared were made to simplify the calculations. Of course, more realistic models should include scattering effects as well as allowing for departures from spherical symmetry. Furthermore, since the opacity from each point out along the ray to the surface can also be found, it is straightforward in principle to compute the net surface brightness by numerical quadrature. Numerical convergence can be checked by refining the discretization interval. In the most demanding models, those with centrally peaked density distributions, satisfactory results were obtained by using 10-point Gaussian quadrature in up to 10 subintervals; in uniform-density models, this was relaxed to four-point Gaussian quadrature. Similar subdivision was used for the quadrature scheme to compute the strip brightness distribution, though a somewhat finer mesh was required to treat the rapidly changing surface brightness in the central region. Subsequently the light curve during a lunar occultation was predicted, using appropriate integrals of the strip brightness distribution over the visible portion of the envelope. These results were normalized by the total flux for display. An independent check of the total flux was made by integration over concentric annuli, the most efficient way to find the spectrum. Fringe visibilities were obtained by using a 32-point complex Fourier transform which exploited the real and symmetrical properties of the strip brightness distribution. The obscured central point source is of negligible importance in the models to be presented. In practice the outer portion of the source contributing less than 3×10^{-3} of the flux was excluded from the mesh. The fringe visibilities were normalized by that at zero spacing; this normalization factor is a third independent estimate of the total flux, and so provides a useful measure of numerical accuracy.

We note that a linear scale can be assigned to the separation of the interferometer elements simply by specifying the angular size, the same observable relevant in occultation measurements. Similarly, separate choices of stellar diameter and distance (and hence intrinsic luminosity) are not necessary for predictions of the flux observed.

Before exploring the properties of a large variety of circumstellar envelopes, we shall describe the results of a comparison by which we investigated the accuracy of our computation. The "standards" were the "graphite" models by Jones and Merrill (1976) for which the temperature distributions were clearly displayed (their Fig. 3). In the case with uniform density, our predicted spectrum was in excellent agreement with theirs. However, in the centrally peaked model (r^{-2} density distribution), our spectrum appears shifted somewhat toward longer wavelengths. We have concluded that while their iterative technique converges on a temperature distribution which conserves flux, the details of the spectral dependence are not entirely consistent. That this is most evident in the centrally peaked model is not surprising, because there is not adequate treatment of the strong peaking of the radiation field in the outward direction, and because the demands for fine radial and frequency meshes are more exacting.

III. SOME REPRESENTATIVE RESULTS

The following models have several features in common. In the center is a star with angular diameter 5.68×10^{-2} arcseconds and effective temperature 2000 K. (At 200 pc this would correspond to a stellar radius of 1220 $R_\odot$ and luminosity 2.13×10^4 $L_\odot$.) The grains are taken to be small compared with the infrared wavelengths considered, and produce a λ^{-2} opacity near 10 μm, somewhat like graphite. A

condensation temperature of 1600 K is assumed. Other features vary from model to model. An outer cutoff to the envelope was defined by the ratio R of the outer to inner radius. Within the envelope the radial density distribution decreases as r^{-n}, with either $n = 0$ (uniform model), or $n = 2$ (centrally peaked model). The actual space density is set by the radial optical depth, characterized here by τ_{10} at 10 μm.

The temperature distributions are chosen to mimic the behavior of published results, fall below the optically thin limit, and preserve flux adequately (Fig. 1). On the other hand, they are somewhat arbitrary in depending on R but not τ or n. Nevertheless, the qualitative conclusions we wish to emphasize are not affected.

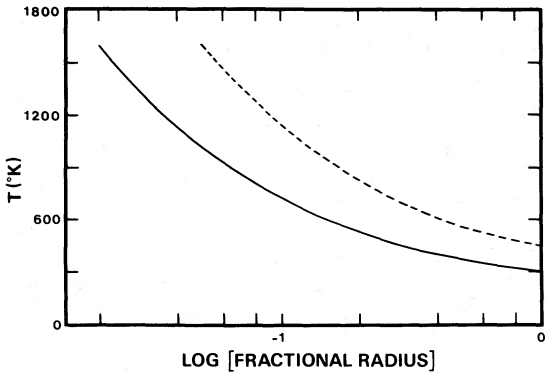

FIG. 1a

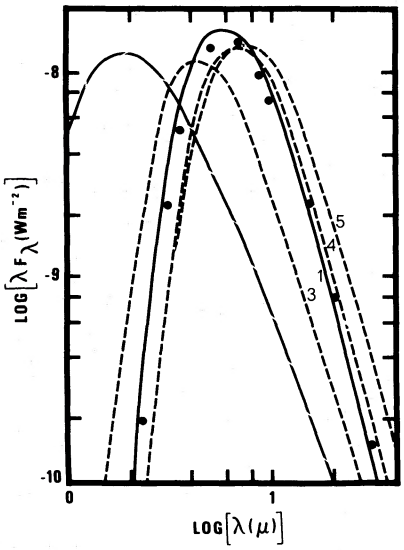

FIG. 1b

FIG. 1.—(*a*) The temperature distributions for the two grids of models with different values of R, the ratio of the outer to inner radius. The solid line represents the models with $R = 50$, while the dashed line shows the temperature distributions for the $R = 20$ models. (*b*) Model emergent spectra (star plus shell) calculated for a range of shell parameters. The long dashed curve represents the spectrum of the underlying star. Each model is characterized by three parameters; τ_{10}, the optical depth at 10 μm; the index n (density $\propto r^{-n}$); and R, the ratio of the outer to inner radius. The 0.3, 0, 20 (τ_{10}, n, R) model (1) is represented by the solid line, while the dots represent the 2.0, 2, 20 model (2). The 0.3, 2, 50 (3), the 2.0, 2, 50 (4), and the 0.3, 0, 50 (5) models are each represented by a short dashed line.

To come directly to our point about the value of occultation or interferometer observations, we present the results for two very different models, both with $R = 20$, but with the combination τ_{10}, n being 0.3, 0 (model 1) and 2, 2 (model 2), respectively. As is seen in Figure 1, the spectra are quite similar in the range 2–30 μm. However, at 10 μm the light curves and fringe visibilities are markedly different, as displayed in Figure 2. The origin of the observed radiation is more centrally concentrated in the $n = 2$ model, and so the light curve is steeper, and the visibility falls less rapidly with element separation.

It is important to make observations at several wavelengths, as examination of the model results for 5 μm (Fig. 3) will demonstrate. In the uniform low-optical-depth model there is relatively greater central peaking at this shorter wavelength, as might be expected on the basis of the temperature gradient. However, the high optical depth in the other model reverses this behavior.

Other model results displayed in Figures 1 and 4 show the effects of increasing R to 50 and, for $R = 50$, of changing either n or τ_{10}. The systematic changes are those expected qualitatively.

IV. IRC +10216

The spatial extent and structure of the luminous infrared source IRC +10216 have been studied by both lunar occultation (Toombs *et al.* 1972) and interferometry (McCarthy and Low 1975; McCarthy, Low, and Howell 1977). These observations have been modeled previously by the combination of two uniformly bright disks, an optically thick, 0.″4 diameter, 600 K component and an optically thin, 2″, 375 K component. Because this simplistic picture seems unlikely to represent the actual physical situation, we have attempted to develop an alternative, more quantitative, model better suited to the quality of the observations. While we are able to present such a model, we cannot claim uniqueness. However, by this example we hope to encourage more realistic modeling of circumstellar envelopes.

Near-infrared spectra indicate a late-type carbon star (Herbig and Zappala 1970); we have accordingly used a temperature of 2000 K. The choice of angular size of the star, the same as in the above models, ensures that the total luminosity, when thermalized to longer infrared wavelengths because of the high optical depth, is adequate to explain the observed flux. (At the suggested distance of 290 pc the luminosity would be $4.5 \times 10^4\ L_\odot$.) Observations of the extended molecular cloud surrounding IRC +10216 seem consistent with a constant outflow velocity and an r^{-2} density distribution (Morris 1975; Kuiper *et al.* 1976). More recent measurements of CO in its first excited vibrational state, which probe into a few stellar radii, indicate that this envelope model holds there as well (Scoville and Solomon 1978). Thus our model is characterized by $n = 2$, together with a condensation

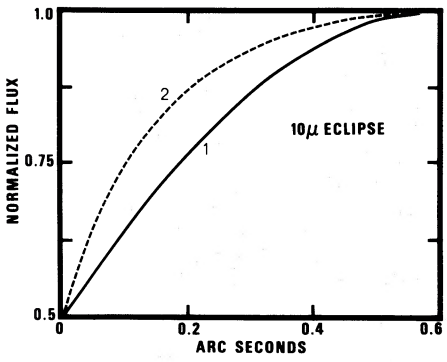

FIG. 2a

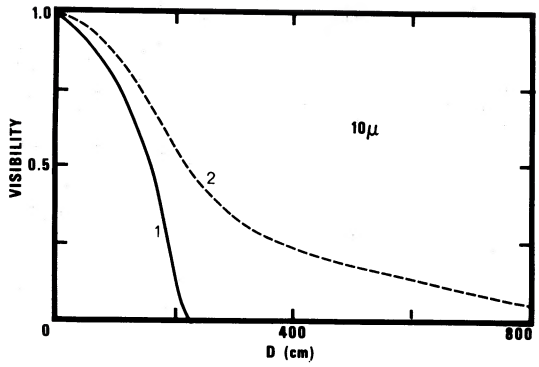

FIG. 2b

FIG. 2.—(*a*) The calculated eclipse data at 10 μm for two models which exhibit similar spectra. The results for model 1 are indicated by the solid line, while the dashed line represents model 2. (See Fig. 7 for some complete curves.) (*b*) The computed fringe visibilities at 10 μm versus baseline for models 1 and 2.

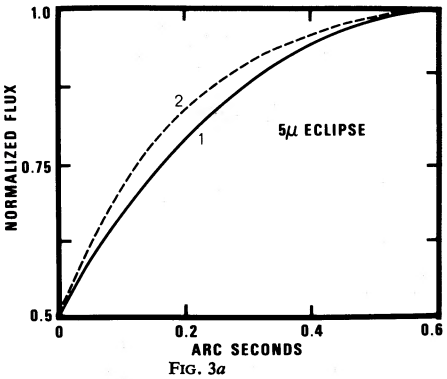

FIG. 3a

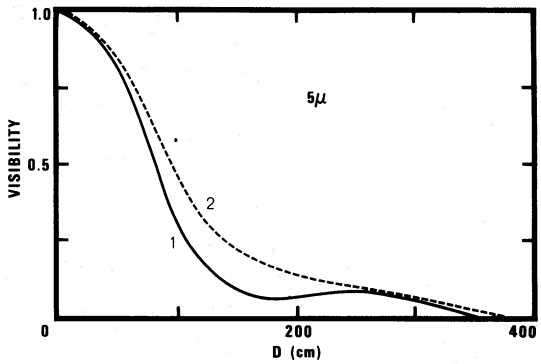

FIG. 3b

FIG. 3.—(*a*) The same as Fig. 2*a*, except for 5 μm. (*b*) The same as Fig. 2*b* except for 5 μm.

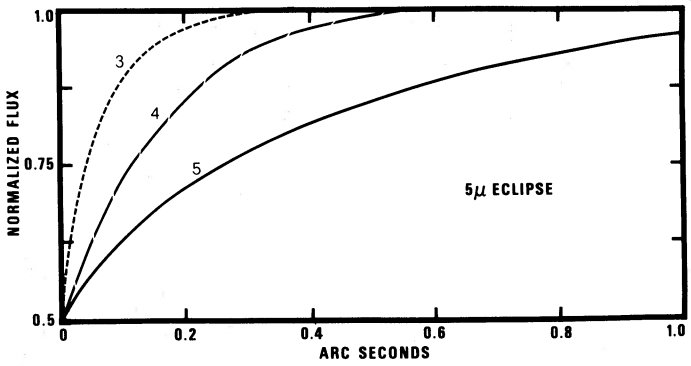

FIG. 4a

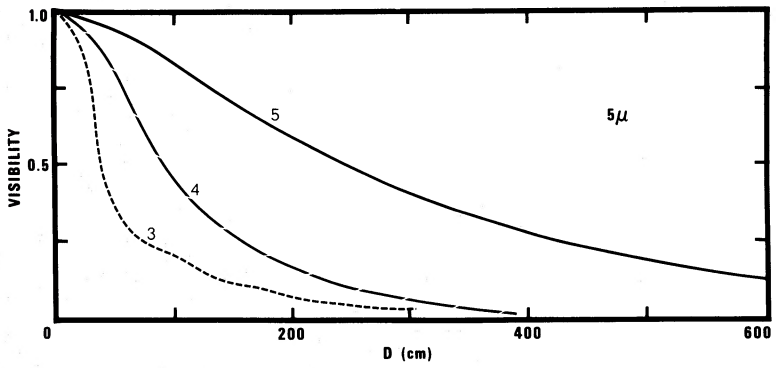

FIG. 4b

FIG. 4.—(*a*) The calculated eclipse data at 5 μm for models 3, 4, and 5 represented by the short dashed, long dashed, and solid lines, respectively. (*b*) The computed fringe visibilities at 5 μm for models 3, 4, and 5.

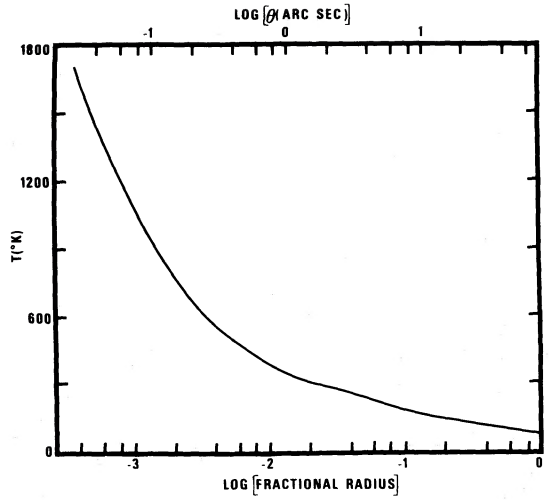

FIG. 5.—The temperature distribution for the model of IRC +10216. The kink at fractional radius (85/2500) is a result of the formulation of the temperature law.

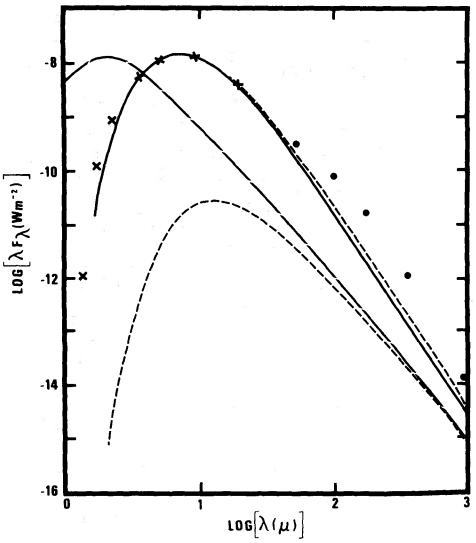

FIG. 6.—The model emergent spectrum of IRC +10216 compared with the observations. The long dashed line is the spectrum of the underlying star, while the lower short dashed line represents the star's contribution to the total flux. The solid line is the emergent spectrum of the model with $R = 85$. The short dashed line indicates the change in the spectrum if R is increased to 2500. The observations of Becklin *et al.* (1969) are indicated by crosses and those of Campbell *et al.* (1976) in the far-infrared by dots.

temperature of 1700 K which implies grain formation very close to the stellar photosphere. We have used a λ^{-1} dependence for the opacity, a rather flat behavior suggested by the slow falloff of the spectrum beyond 50 μm (Campbell *et al.* 1976). (In a complete analysis one would want to consider the implications of this opacity law for the grain composition and size distribution, and the attendant effects on the temperature distribution. The possibility of the coexistence of several grain types with different temperature distributions should also be entertained; there is spectral evidence at 11.3 μm for SiC grains.) Finally, the model was taken to be sufficiently extensive that truncation of the density distribution produced no observable effect; in the model presented it was established that $R = 2500$ was quite suitable, by comparison with results for $R = 85$. The temperature distribution of the model is shown in Figure 5; the kink at fractional radius 85/2500 is an artifact of our

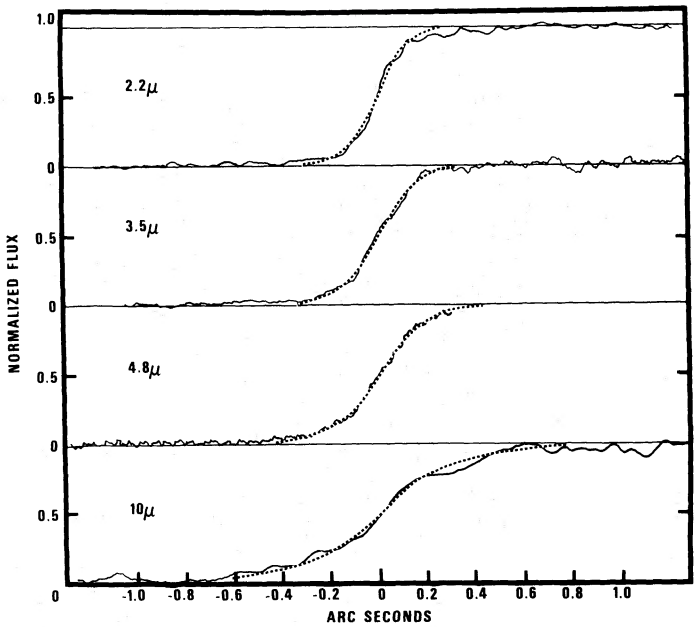

FIG. 7.—The simulated eclipse observations at several wavelengths compared with the observations of Toombs *et al.* (1972)

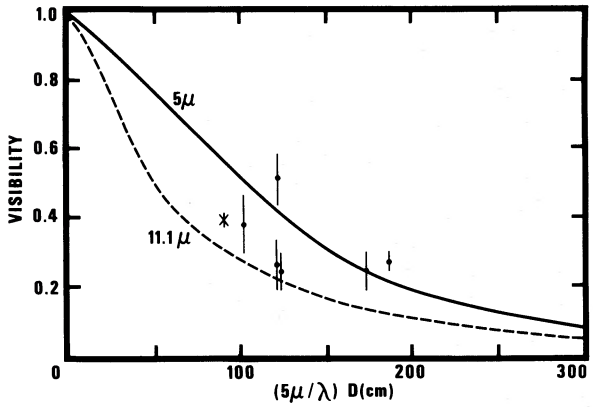

FIG. 8.—The fringe visibilites as computed from the model for 5 μm (*solid*) and 11.1 μm (*dashed*). The visibilities have been plotted against baseline normalized to 5 μm, i.e., the same angular scale. The dots represent the observations of McCarthy and Low (1975) at all position angles. The observation of McCarthy *et al.* at 11.1 μm is indicated by the asterisk.

formulation of the temperature law and has no bearing on the results.

Having made all of these preliminary specifications, we had only one adjustable parameter, the optical depth. After only a few trials it was found that $\tau_{10} = 3.3$ ($R = 85$; $\tau_{10} = 3.34$ when $R = 2500$) provided a good approximation to the observed spectrum, as displayed in Figure 6. The characteristics that are matched by this preliminary model are the wavelength and level of the maximum, and the width of the spectral distribution. However, at wavelengths beyond 100 μm the prediction is as much as a factor 3 too low. We decided that tinkering with the many adjustable parameters to provide a better fit would not be justifiable, and so proceeded to predict the eclipse light curves and the fringe visibilities.

The light curves are compared with the observations in Figure 7, where it can be seen that the agreement is remarkably good. The model not only predicts the characteristic size decrease at short wavelengths but also has the correct absolute scale. Although we regard the detailed agreement as fortuitous, we are satisfied that the global characteristics of the model have been demonstrated to be reasonable. Finally, the fringe visibility at 5 μm is examined in Figure 8. Again the agreement is good. This incidentally also shows that the eclipse and interferometer results are reasonably consistent, as modeling with uniform disks has already suggested. However, the one measurement at 11 μm falls above our prediction.

Underlying our model is an assumption that material has been streaming from the star at velocity 12 km s^{-1} with a steady rate for at least 7.9×10^3 (d/290 pc)(θ/2.″3) yr. The latter estimate is the expansion time to the observed diameter of the extended CO cloud (Wilson, Schwartz, and Epstein 1973). Other molecules are seen in a more central, warmer part of this flow; further in still, the infrared emission arises. However, there are no distinct boundaries between these regions in our model. We are intrigued that the 0.″4 and 2″ components used by Toombs *et al.* (1972) to model their data conveniently have been used so often in subsequent interpretations of other infrared and molecular line data. Although this two-component model provides a useful device from which other characteristics of the source can be computed, the initial success of our model suggests that the two components need not really be regarded as distinct, or as possessing special evolutionary status such as discrete outbursts. Obviously our "single"-component model suggests a different evolutionary history for IRC +10216 from that implied by a two-component model.

To compute mass-related properties of our model, we took the mass-absorption coefficient to be 4.8×10^3 cm^2 g^{-1} at 2.3 μm, which is appropriate to small particles of graphite (Jones and Merrill 1976). The adopted λ^{-1} dependence implies 100 cm^2 g^{-1} at 100 μm, much above that for pure graphite but possibly consistent with an impure material. The total column density of dust across the diameter of the source is therefore 6×10^{-3} g cm^{-2}, independent of distance. The steady mass-loss rate in dust alone is 9×10^{-8} (d/290 pc) $M_\odot$ yr^{-1}, which over the lifetime of the source amounts to 7×10^{-4} (d/290 pc)^2(θ/2.″3) $M_\odot$. As Campbell *et al.* (1976) have pointed out, these are comparable with corresponding values for heavy molecules. If we scale these numbers up by about a factor 10^2–10^3, to include H_2, the envelope has a total mass of 0.14–1.4 $M_\odot$. A consistent model of IRC +10216 as an early stage in the development of a planetary nebula is therefore possible.

This research was supported by the National Research Council of Canada and a Carl Reinhardt Fellowship to one of us (D. R. C.).

REFERENCES

Apruzese, J. P. 1974, *Ap. J.*, **188**, 539.
———. 1975, *Ap. J.*, **196**, 761.
Becklin, E. E., Frogel, J. A., Hyland, A. R., Kristian, J., and Neugebauer, G. 1969, *Ap. J.* (*Letters*), **158**, L133.
Bergeat, J., Lefevre, J., Kandel, R., Lunel, M., and Sibille, F. 1976, *Astr. Ap.*, **52**, 245.
Campbell, M. F., *et al.* 1976, *Ap. J.*, **208**, 396.
Feast, M. W., and Glass, I. S. 1973, *M.N.R.A.S.*, **161**, 293.
Herbig, C. H., and Zappala, R. R. 1970, *Ap. J.* (*Letters*), **162**, L15.
Jones, T. W., and Merrill, K. M. 1976, *Ap. J.*, **209**, 509.
Kuiper, T. B. H., Knapp, G. R., Knapp, S. L., and Brown, R. L. 1976, *Ap. J.*, **204**, 408.
McCarthy, D. W., and Low, F. J. 1975, *Ap. J.* (*Letters*), **202**, L37.
McCarthy, D. W., Low, F. J., and Howell, R. 1977, *Ap. J.* (*Letters*), **214**, L85.
Michelson, A. A., and Pease, F. G. 1921, *Ap. J.*, **53**, 249.
Morris, M. 1975, *Ap. J.*, **197**, 603.
Robinson, G., and Hyland, A. R. 1977, *M.N.R.A.S.*, **180**, 495.
Scoville, N. Z., and Solomon, P. M. 1978, *Ap. J.* (*Letters*), **220**, L103.
Sutton, E. C., Storey, J. V. C., Betz, A. L., Townes, C. H., and Spears, D. L. 1977, *Ap. J.* (*Letters*), **217**, L97.
Taam, R. E., and Schwartz, R. D. 1976, *Ap. J.*, **204**, 842.

Toombs, R. I., Becklin, E. E., Frogel, J. A., Law, S. K., Porter, F. C., and Westphal, J. A. 1972, *Ap. J.* (*Letters*), **173**, L71.
Wilson, W. J., Schwartz, P. R., and Epstein, E. E. 1973, *Ap. J.*, **183**, 871.
Woolf, N. J., 1973, in *IAU Symposium No. 52, Interstellar Dust and Related Topics*, ed. J. M. Greenberg and H. C. van de Hulst (Dordrecht: Reidel), p. 485.
Zappala, R. R., Becklin, E. E., Matthews, K., and Neugebauer, G. 1974, *Ap. J.*, **192**, 109.

DENNIS R. CRABTREE and P. G. MARTIN: Department of Astronomy, University of Toronto, Toronto, ON, M5S 1A7, Canada